



# Brain activity during intraoperative general anesthesia using resting-state functional magnetic resonance imaging ~ Feasibility study ~

Junji Wakabayashi<sup>1</sup> · Yoshitetsu Oshiro<sup>1</sup> · Shigeyuki Kan<sup>2</sup> · Masaaki Kohta<sup>3</sup> · Masaaki Taniguchi<sup>3,4</sup> · Norihiko Obata<sup>1</sup> · Masako Okada<sup>1</sup> · Eiji Kohmura<sup>3,5</sup> · Takashi Sasayama<sup>3</sup> · Satoshi Mizobuchi<sup>1</sup>

Received: 25 August 2024 / Accepted: 24 February 2025 / Published online: 31 March 2025  
© The Author(s) under exclusive licence to Japanese Society of Anesthesiologists 2025

## Abstract

**Background** In recent years, the effects of general anesthetics on the brain have been widely studied at the sedation level using resting-state functional magnetic resonance imaging (rs-fMRI). Most anesthesia protocols use a single agent, and changes in spontaneous brain activity are examined to show the characteristics of each anesthetic agent. However, no studies have used rs-fMRI to evaluate the effects of anesthesia during actual surgery. We examined the feasibility of evaluating the effects of general anesthesia with sevoflurane using rs-fMRI during neurosurgery.

**Methods** We enrolled 20 adult patients scheduled for transsphenoidal surgery. We compared differences between before and during general anesthesia in terms of brain functional connectivity of the thalamus by seed-to-voxel correlation analysis and local neural activity using fractional amplitude of low-frequency fluctuations (fALFF) analysis. An exclusion mask was applied to exclude brain areas showing intraoperative spatial artifacts and correct for differences in the magnitude of intra- and preoperative head movements.

**Results** We analyzed 16 patients. Functional connectivity of the thalamus to the contralateral thalamus, bilateral caudate nucleus and globus pallidus were significantly decreased during anesthesia. The precuneus and posterior cingulate cortex showed significantly decreased fALFF values during anesthesia.

**Conclusion** These findings were consistent with previous studies and indicate the feasibility of intraoperative rs-fMRI during general anesthesia.

**Keywords** Functional connectivity · Functional MRI · General anesthesia · Intraoperative neurophysiological monitoring · MR

## Introduction

In recent years, the effects of general anesthetics on the brain have been widely studied at the sedation level using resting-state functional magnetic resonance imaging (rs-fMRI) [1–4]. Most anesthesia protocols use a single agent, and changes in spontaneous brain activity are examined to show the characteristics of each anesthetic agent. However, no studies have used rs-fMRI to evaluate the effects of anesthesia during actual surgery.

Evaluation of spontaneous brain activity during general anesthesia using intraoperative rs-fMRI may be very useful in characterizing the changes that occur in the brain under the influence of multiple drugs during general anesthesia. We therefore examined the feasibility of evaluating the effects of general anesthesia (mainly from sevoflurane) on

✉ Junji Wakabayashi  
oo22ver@yahoo.co.jp

<sup>1</sup> Department of Anesthesiology, Kobe University Graduate School of Medicine, 7-5-1, Kusunoki-Cho, Chuo-Ku, Kobe, Hyogo Zip Code: 650-0017, Japan

<sup>2</sup> Research Organization of Science and Technology, Ritsumeikan University, Kusatsu, Shiga, Japan

<sup>3</sup> Department of Neurosurgery, Kobe University Graduate School of Medicine, Kobe, Hyogo, Japan

<sup>4</sup> Department of Neurosurgery, Osaka Neurological Institute, Toyonaka, Osaka, Japan

<sup>5</sup> Department of Neurosurgery, Kinki Central Hospital, Itami, Hyogo, Japan

the brain, and the thalamus in particular, using rs-fMRI during neurosurgery.

## Methods

### Design and ethics

This study used a single-center, prospective, observational design. This study was approved by the Kobe University Hospital Ethics Committee (approval no. 1787) and was conducted in accordance with the Declaration of Helsinki. Written informed consent was obtained from all participants prior to enrolment.

### Setting and participants

We screened 20 adult patients scheduled for elective transphenoidal surgery in the study site from December 2015 to April 2019. None of these 20 patients had any disturbance of consciousness preoperatively as of the date of admission (1–3 days before surgery). Among these, we enrolled those patients who were scheduled for intraoperative MRI to evaluate the progress of surgery. Patients with valid scans less than 90% of all scans, maximum body motion values greater than 3 mm, and average body motion values greater than 1 mm were excluded from the analysis of this study.

### Anesthetic management during operation and fMRI

All patients were anesthetized with propofol, midazolam, sevoflurane, fentanyl, remifentanyl, and rocuronium before intraoperative MRI. Each patient was intubated and received an arterial line. Anesthesia with sevoflurane, fentanyl, and rocuronium was induced using an MRI-compatible anesthetic machine (Aestiva/5 MRI; Datex-Ohmeda, Madison, WI, USA) during the MRI session. We collected data from the electronic medical records, including type and dose of anesthetics, and the timing of administrations before and during the intraoperative MRI session.

### Acquisition of rs-fMRI data

We performed rs-fMRI preoperatively (control) and intraoperatively. Data acquisition was performed using a 3-T MRI scanner (MAGNETOM Skyra 3-Tesla; Siemens Healthineers, Erlangen, Germany). A 20-channel head/neck coil was used for preoperative MRI, and an 8-channel head/holder coil (FLEXIBILITY OR Head Holder & 8-Ch Coil; NORAS MRI products, Hoechberg, Germany) was used for intraoperative MRI. Prior to performing preoperative rs-fMRI, each patient was given the following instructions: “Close your eyes, relax, and do not think of anything in

particular. Do not fall asleep.” Intraoperative imaging was performed after the completion of tumor removal under general anesthesia. Functional images were acquired using a gradient-echo echo-planar imaging sequence with two slightly different parameters (in this study, two different data sets were used for analysis). For Patients 1–9, the following parameters were applied: repetition time, 2530 ms; echo time, 30 ms; flip angle, 80°; voxel size, 3.75 × 3.75 × 3.0 mm<sup>3</sup> with 0.6-mm gap; images, 150. For Patients 10–16, the parameters applied were: repetition time, 2000 ms; echo time, 30 ms; flip angle, 90°; voxel size, 3.75 × 3.75 × 3.0 mm<sup>3</sup> with 0.6-mm gap; images, 300 (the first 150 images were used for analysis). Anatomical images were acquired using a T1-weighted three-dimensional (3D) magnetization-prepared rapid acquisition with gradient echo sequence. For the preoperative scan, the following parameters were used: repetition time, 2300 ms; echo time, 2.3 ms; flip angle, 8°; sagittal slices, 192; voxel size, 1 × 1 × 1 mm<sup>3</sup>. For the intraoperative scan, the following parameters were used: repetition time, 2300 ms; echo time, 2.3 ms; flip angle, 8°; sagittal slices, 512; voxel size, 0.5 × 1.0 × 1.0 mm<sup>3</sup>.

### Analysis of rs-fMRI data

Preprocessing procedures were performed using the CONN functional connectivity toolbox (version 17.f; [www.nitrc.org/projects/conn](http://www.nitrc.org/projects/conn)) and SPM12 (version 7771; [www.fl.ion.ucl.ac.uk/spm/](http://www.fl.ion.ucl.ac.uk/spm/)). Briefly, functional magnetic resonance (fMR) images of each patient were first realigned (motion correction) and corrected for slice acquisition timing (slice timing correction). Functional and structural images were normalized to Montreal Neurological Institute templates of echo-planar images and 3D T1-weighted images followed by nonlinear transformation, respectively. Finally, images were smoothed with a Gaussian kernel of 8 mm at full width at half maximum. In individual analyses, we performed seed-to-voxel correlation analysis. Before functional connectivity (FC) and fractional amplitude of low-frequency fluctuations (fALFF) analysis, we performed band-pass filtering (band-pass frequency, 0.008–0.09 Hz) and linear regression to remove noise components from fMRI signals, such as non-neural physiological noise components derived from aCompCor [5], head motion, and low-frequency drift. To make individual FC and fALFF maps, we performed seed-based FC analysis and fALFF analysis for each patient. These maps were used for second-level between-condition comparisons.

The seeds used for FC analysis were the left and right thalamus, as previous reports have noted that the loss of consciousness resulting from induction of anesthesia was related to declines in FC between the thalamus and cortex [6], and declines in thalamic activity [7].

We also performed fALFF analysis to investigate differences in the degree of local neural activity between pre- and intraoperative conditions [8].

### Spatial artifacts on intraoperative fMRI and masking

The following three types of spatial artifacts were observed on intraoperative fMRI (Fig. 1). The first type was head fixation pin artifacts, representing artifacts around the pins used to fixate the head during surgery. The second type was air artifacts, representing artifacts around the air that enters the skull. The third type was off-center artifacts (field inhomogeneity artifacts or susceptibility artifacts caused by an off-center position on the gantry), representing artifacts caused by the head fixation position being off the center of the gantry due to the surgical procedure.

Signal loss on fMRI due to these artifacts covers a large number of regions, and masking was performed to exclude these regions from analysis (Fig. 1).

SPM12 was used to create the exclusion mask by superimposing extracted images of the areas showing signal loss in the functional images for each patient, and excluding those areas found to show signal loss in more than four patients (Supplementary Fig. 1).

The present study compared FC strength and fALFF values taken preoperatively in a resting, eyes-closed condition with those taken intraoperatively under general anesthesia. Preoperative rs-fMRI data with eyes closed at rest were

affected by head movements, such as swallowing, that are seen in an awake state, but intraoperative data under general anesthesia were unaffected by such head movements. We therefore corrected for differences in head motion to cancel head movement effects on FC strength and fALFF values.

To evaluate the effects of head movements, we compared pre- and intraoperative head movements based on framewise displacement (FD) [9]. We then calculated the difference between pre- and intraoperative FD values for each subject by averaging the FD values for each subject detected by CONN. The difference in FD values between the pre- and intraoperative rs-fMRI data was used for paired t-tests as a covariate (or a nuisance regressor), correcting for the influence of head motion.

### Statistical analysis

Paired t-testing was performed to investigate differences in brain FC and fALFF between pre- and intraoperative conditions. In all comparisons of FC strength between pre- and intraoperative conditions, the significance level was  $p < 0.001$  (uncorrected for multiple comparisons) at the voxel level and  $p < 0.05$  (family-wise error [FWE]-corrected) at the cluster level. Moreover, Bonferroni correction for multiple comparisons was applied to the cluster-level threshold because the left and right thalamus were seeds. Thus, an FWE-corrected value of  $p < 0.025$  ( $0.05/2$ ) was required for a statistically significant result. In the comparison of fALFF between pre- and

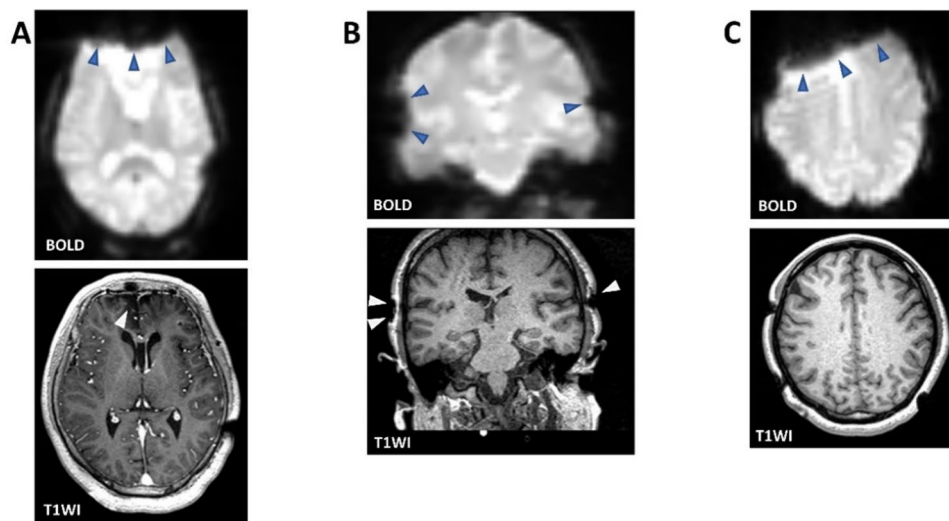


**Fig. 1** Spatial artifacts on intraoperative functional magnetic resonance (fMR) images. Upper images are fMR images and lower images are 3-dimensional (3D) T1-weighted structural images (T1WI) corresponding to the same slice as the upper images. **A** An example of air (susceptibility) artifacts: blue arrows on fMR images indicate susceptibility artifacts caused by intracranial air, and the white arrows on 3D T1WI indicate intracranial air. **B** An example of head fixation pin (metal) artifacts: blue arrows indicate metal arti-

facts due to the cranial fixation device, and white arrows indicate the defect in the scalp from the cranial fixation device. **C** An example of off-center artifacts: blue arrows show off-center artifacts caused by magnetic field inhomogeneity at off-center locations. In contrast, no distortion is evident on 3D T1WI. The difference between the two images results from the fact that echo-planar images are more vulnerable to magnetic field inhomogeneity

intraoperative conditions, the significance level was  $p < 0.001$  (uncorrected for multiple comparisons) at the voxel level and  $p < 0.05$  (FWE-corrected) at the cluster level. We performed these statistical analyses using SPM12.

## Results

During the study period, 20 adult patients underwent intraoperative rs-fMRI during elective transsphenoidal surgery. We excluded 1 patient who was lacking an accurate anesthesia record during intraoperative fMRI and 3 patients showing motion artifacts in MRI signals. Eventually, we analyzed rs-fMRI data from 16 patients.

### Characteristics of patients

Analyzed data were acquired from 8 women and 8 men with a mean age of 49 years (range, 21–76 years). The underlying pathology in these patients was pituitary adenoma in 9 patients, craniopharyngioma in 2 patients, and Rathke's cleft cyst, chondrosarcoma, sebaceous carcinoma, fibrous dysplasia and suspected hypophysitis in 1 patient each (Table 1).

### Management of anesthesia

Table 1 shows the anesthetic agents used before and during intraoperative MRI. Four patients (Patients 2, 8, 9, and 15) were anesthetized using propofol (target-controlled infusion) and all others were anesthetized using sevoflurane before the intraoperative MRI session. The effect-site concentration of propofol, the inspired sevoflurane concentration, and the dose of remifentanyl administered just before intraoperative MRI were 2.3–3.6  $\mu\text{g/ml}$  (mean, 2.93  $\mu\text{g/ml}$ ), 1–3% (mean, 1.83%), and 0.05–0.3  $\mu\text{g/kg/min}$  (mean, 0.177  $\mu\text{g/kg/min}$ ), respectively. The total dose of fentanyl administered before the intraoperative MRI session was 1.96–10.57  $\mu\text{g/kg}$  (mean, 6.11  $\mu\text{g/kg}$ ). Only Patient 2 was administered 2 mg (0.031 mg/kg) of midazolam intravenously.

All patients were anesthetized with sevoflurane during the intraoperative MRI session. Half of the patients (Patients 1, 2, 4, 6, 7, 12, 13, and 16) were administered fentanyl during the intraoperative MRI session, but the others were not. The inspired sevoflurane concentration and total dose of fentanyl administered during intraoperative MRI were 1.5–3% (mean, 2.05%) and 0.83–2.41  $\mu\text{g/kg}$  (mean, 1.66  $\mu\text{g/kg}$ ), respectively.

### Comparisons of FC involving the thalamus between pre- and intraoperative conditions, and effects of FD correction and spatial artifact masking

FC strengths of the right thalamus with the contralateral thalamus, bilateral caudate nucleus, and globus pallidus

were significantly decreased during anesthesia without FD correction (Fig. 2A, Table 2). In contrast, FC strengths of the right thalamus with the operculum, insula, parahippocampal gyrus, hippocampus, and fusiform gyrus were significantly increased during anesthesia without FD correction (Fig. 2B, Table 2). However, after FD correction, differences in FC strength between the two conditions decreased. As a result, the region in which FC decreased during anesthesia was reduced in size (Fig. 2C, Table 2), and clusters with increased FC strength during anesthesia no longer showed significant differences (Fig. 2D, Table 2). In addition, the application of the exclusion mask partially excluded the region in which FC decreased during anesthesia (Fig. 2E, Table 2). Almost no differences in the results of FC of the thalamus were seen between the left and right sides (Supplementary Fig. 2).

### Comparisons of fALFF between pre- and intraoperative conditions, and effects of FD correction and masking

The thalamus, precuneus, posterior cingulate cortex (PCC), supramarginal gyrus, lingual gyrus, occipital pole, lateral occipital cortex, and postcentral gyrus showed significantly decreased fALFF values during anesthesia (Fig. 3A, Table 3). In contrast, fALFF values were significantly increased in the temporal pole, middle temporal gyrus, inferior temporal gyrus, fusiform gyrus, frontal pole, several parts of the cerebellum, and left orbitofrontal cortex during anesthesia (Fig. 3B, Table 3). However, after FD correction, the extent of significant clusters was markedly decreased (Fig. 3C, D, Table 3). Conversely, no differences were seen in the results of the fALFF analysis, regardless of the application of the exclusion mask (Fig. 3E, F, Table 3).

## Discussion

In this study, rs-fMRI was performed during transsphenoidal surgery under general anesthesia (mainly with sevoflurane), and FC and fALFF with the thalamus were compared between anesthesia and wakefulness. In these analyses, differences in the magnitude of body movements between awake and anesthetized patients were corrected based on differences in mean frame displacement. In addition, spatial artifacts due to intraoperative conditions were observed in rs-fMRI during surgery, and an exclusion mask was created and applied to minimize the effects of these artifacts.

This study showed that intra- and interthalamic FC and FC between the thalamus and basal ganglia both decreased during anesthesia. In addition, this study showed that fALFF values in the precuneus and PCC decreased during anesthesia. Application of body motion correction and the spatial

**Table 1** Characteristics of patients and anesthetic data

Characteristics		Anesthetic data												
ID	Sex	Age (years)	ASA-PS	Target disease	Before intraoperative MRI session					During intraoperative MRI session				
					Propofol TCI (µg/ml)	Inspired sevo concentration (%)	Remifentanyl dose (µg/kg/min)	Fentanyl dose (µg/kg)	BIS value	Inspired sevo concentration (%)	Fentanyl dose (µg/kg)	BIS value	Inspired sevo concentration (%)	Fentanyl dose (µg/kg)
1	M	58	2	Rathke's cleft cyst	N/A	1.4	0.15	3.83	N/A	2	1.53			
2	F	49	1	Pituitary adenoma	2.3	2.5	0.3	7.58	N/A	3	1.52			
3	F	42	2	Pituitary adenoma	N/A	1.5	0.17	1.96	N/A	1.5	N/A			
4	M	21	2	Craniopharyngioma	N/A	1.5	0.3	10.46	N/A	2	2.2			
5	M	63	2	Craniopharyngioma	N/A	2	0.1	3.46	N/A	3	N/A			
6	M	35	1	Fibrous dysplasia	N/A	2.5	0.15	5.17	N/A	3	1.29			
7	M	68	2	Pituitary adenoma	N/A	1	0.15	9.64	N/A	2	2.41			
8	F	57	2	Pituitary adenoma	2.8	2	0.2	10.57	N/A	2	N/A			
9	F	28	2	Pituitary adenoma	3	3	0.25	7.1	N/A	2.5	N/A			
10	M	61	2	S/o hypophysitis	N/A	1.6	0.05	6.62	48	1.6	N/A			
11	F	31	1	Pituitary adenoma	N/A	1.6	0.15	4.9	41	1.6	N/A			
12	F	40	1	Pituitary adenoma	N/A	1.8	0.16	4.16	49	1.8	0.83			
13	M	76	2	Sebaceous carcinoma	N/A	1.5	0.1	5.22	44	1.5	1.49			
14	M	58	1	Chondrosarcoma	N/A	1.5	0.25	3.81	62	1.5	N/A			
15	F	72	2	Pituitary adenoma	3.6	1.8	0.25	N/A	53	1.8	N/A			
16	F	27	1	Pituitary adenoma	N/A	2	0.1	7.14	48	2	2.04			

\* ASA-PS, American Society of Anesthesiologists physical status; TCI, target-controlled infusion; sevo, sevoflurane; BIS, bispectral index; F, female; M, male; N/A, not available; s/o, suggestive of

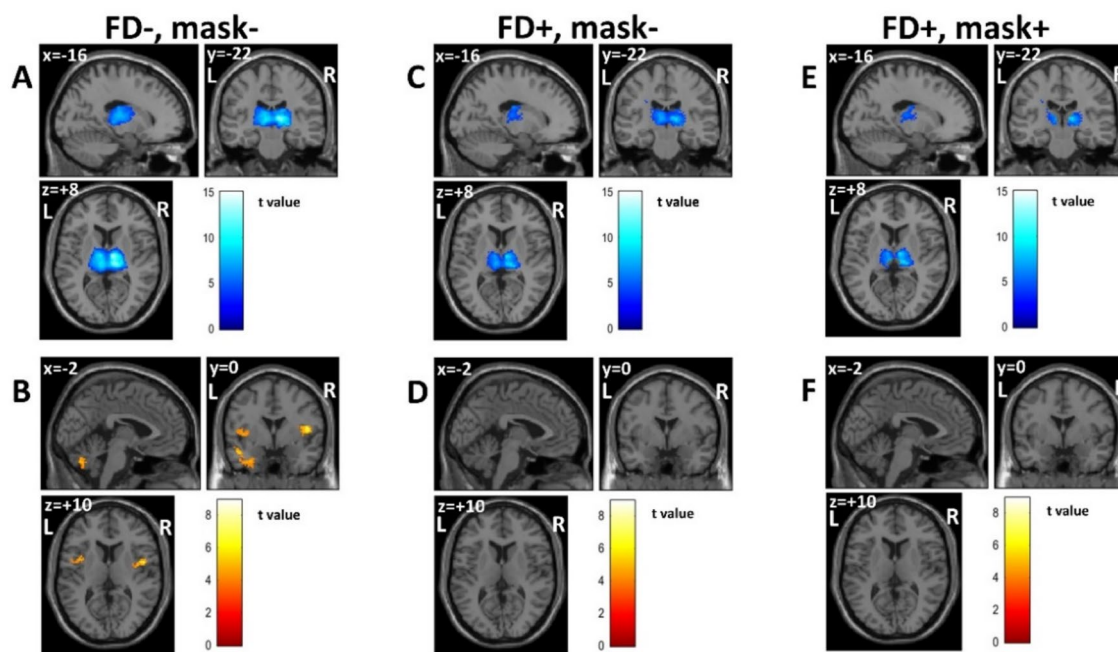


**Fig. 2** Differences in functional connectivity (FC) of the right thalamus before and during anesthesia. **A, C, E** Brain regions showing significant FC decrease during anesthesia (intraoperative MRI). **B, D, F** Brain regions showing significant FC increase during anesthesia. **A, B** FC maps without framewise displacement (FD) correction and the exclusion mask. **C, D** FC maps with FD correction and without

the exclusion mask. **E, F** FC maps with FD correction and the exclusion mask. All FC maps used a threshold of  $p < 0.001$  (uncorrected for multiple comparisons) at the voxel level and  $p < 0.025$  (FWE-corrected) at the cluster level. FD+, FC map with FD correction; FD-, FC map without FD correction; mask+, FC map with the exclusion mask; mask-, FC map without the exclusion mask

artifact exclusion mask to the results of FC and fALFF analysis eliminated some areas that had shown significant differences.

Since the purpose of this study was to compare images taken while awake and during surgery and a state of general anesthesia results in virtually no body movement, the effects of the magnitude of body movement needed to be excluded. Corrections were therefore made based on the difference in mean frame displacement for each subject. FD represents the sum of the magnitude of linear motions of the head in the x, y, and z directions and rotational motion in the three directions, providing an indicator of overall head movements.

Previous reports have evaluated the effects of head movements in neonates [10] and the elderly [11] on rs-fMRI using FD. With this method, we were able to exclude the effects of body motion in the FC and fALFF analyses. In the present study, spatial artifacts caused by the intraoperative condition were observed, resulting in signal loss from functional brain images.

To minimize the effects of artifacts while maintaining detection power, a mask was created and adapted to exclude areas in which artifacts were seen in four or more subjects.

The present study found a decrease in FC within and between the thalamus during anesthesia. These results indicate that sevoflurane anesthesia reduces both neural activity

in the thalamus and interthalamic synchrony. Previous studies on the thalamus and anesthesia have reported that loss of consciousness during anesthesia is associated with hypometabolism in the thalamus, decreased interthalamic FC, or decreased thalamocortical interactions [6, 7, 12, 13]. The results of the present study demonstrate that those findings from previous studies of reduced activity and FC of the thalamus itself in association with anesthesia-induced loss of consciousness are also observed during balanced anesthesia with sevoflurane. One study using electroencephalography (EEG) showed that the waveforms of the left and right cerebral hemispheres became similar under anesthesia. This finding suggests that interthalamic FC increases under anesthesia, which appears inconsistent with our findings. The cause of this inconsistency is unclear but may be attributable to differences in methods of measurement and temporal resolution between fMRI and EEG. Further studies are needed to clarify and validate our results.

In this study, fALFF values in the precuneus and PCC decreased during anesthesia. The PCC and precuneus are components of the default mode network (DMN), which is thought to play an important role in the formation of consciousness. Previous studies on the DMN and anesthesia have shown that anesthesia is related to impaired FC within the DMN [14–16], and decreases both local

**Table 2** Results of functional connectivity (FC) analysis

Comparison	Seed	FD	Mask	Clusters (x, y, z)	Size (voxels)	Peak <i>t</i> value	Brain regions
pre > intra	Right thalamus	-	-	+ 10, - 12, + 6	4105	14.87	Left thalamus, right thalamus, left caudate, right caudate, right pallidum, left pallidum
		+	-	+ 10, - 12, + 6	2368	9.87	Left thalamus, right thalamus, right pallidum, right caudate, left caudate
		+	+	+ 10, - 12, + 6	1586	9.87	Left thalamus, right thalamus, right pallidum, right caudate, left caudate
	Left thalamus	-	-	+ 12, - 24, + 8	3706	14.2	Right thalamus, left thalamus, left pallidum, left caudate, right caudate, left putamen, right pallidum
		+	-	- 8, - 12, + 6	1926	10.68	Right thalamus, left thalamus, right caudate, left pallidum
		+	+	- 8, - 12, + 6	1362	10.68	Right thalamus, left thalamus, left caudate, right pallidum
intra > pre	Right thalamus	-	-	- 30, + 10, - 40	1092	8.91	Left TP, left Cereb45, left posterior TFusC, left posterolateral ITG, left posterior PaHC, left anterior STG, left anterior TFusC, left anterior PaHC, left hippocampus, left PP, left Cereb6, left anterolateral ITG, left amygdala, left anterior MTG, brainstem
				- 44, + 2, + 8	187	5.17	Left IC, left CO, left PreCG, left opercular IFG, left FO, left putamen
				0, - 70, - 38	151	5.67	Ver8, Ver7, right Cereb2, right Cereb7, left Cereb2, right Cereb8, left Cereb8
				+ 46, 0, + 12	146	8.16	Right CO, right IC
	Left thalamus	+	-	No suprathreshold clusters			
		+	+	No suprathreshold clusters			
		-	-	+ 26, - 18, - 32	350	5.74	Right anterior PaHC, right anterior TFusC, right amygdala, right hippocampus, right posterior PaHC, right TP, right FORb, brainstem, right posterior TFusC
				+ 42, + 2, + 10	307	6.91	Right IC, right CO, right FO, right opercular IFG
				- 34, + 14, + 6	223	5.88	Left IC, left FO l, left CO
				- 32, - 38, - 24	172	5.56	Left posterior TFusC, left Cereb45, brainstem, left Cereb6
				- 6, - 62, - 20	136	5.73	Ver8, left Cereb6, Ver6, right Cereb2, Ver7, left Cereb45, left Cereb8, right Cereb7, right Cereb8
	+	-	No suprathreshold clusters				
	+	+	No suprathreshold clusters				

\*PaHC, parahippocampal gyrus; TFusC, temporal fusiform cortex; TP, temporal pole; FORb, frontal orbital cortex; IC, insular cortex; CO, central opercular cortex; FO, frontal opercular cortex; IFG, inferior frontal gyrus; ITG, inferior temporal gyrus; MTG, middle temporal gyrus; STG, superior temporal gyrus; PP, planum polare; PreCG, precentral gyrus; Cereb, cerebellum; Ver, vermis; pre > intra, brain regions that showed significant FC decrease during anesthesia; intra > pre, brain regions that showed significant FC increase during anesthesia; FD, framewise displacement

synchronicity in the DMN [17] and neural activity in the DMN [18, 19]. The present results and findings from those previous studies support the association of reduced activity and FC of the DMN with anesthesia-induced loss of consciousness in humans under anesthesia with sevoflurane.

Previous studies using EEG targeting frontal and parietal activities during general anesthesia surgery have provided a common observation that dominant feedback connectivity in the fronto-parietal network is disrupted during general anesthesia with propofol, sevoflurane, or ketamine [20, 21].

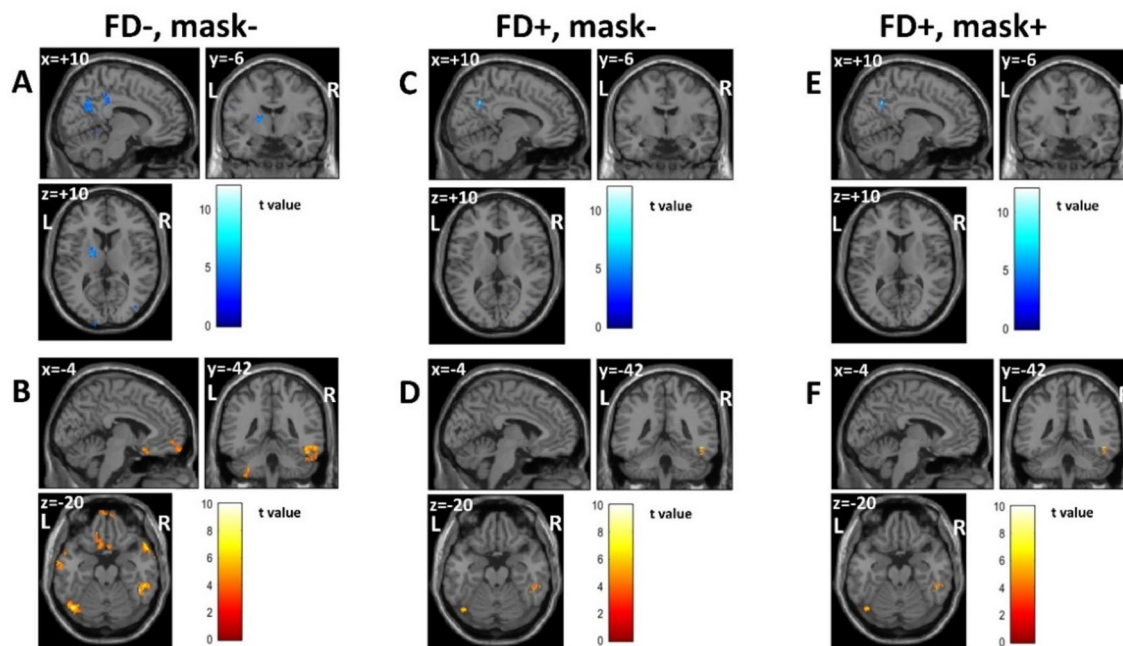


**Fig. 3** Differences in fractional amplitude of low-frequency fluctuation (fALFF) between before (preoperative MRI condition) and during anesthesia (intraoperative condition). **A, C, D** Brain regions showing significant fALFF decrease during anesthesia. **B, D, F** Brain regions showing significant fALFF increase during anesthesia. **A, B** Maps of fALFF without framewise displacement (FD) correction and the exclusion mask. **C, D** Maps of fALFF with FD correction and

without the exclusion mask. **E, F** Maps of fALFF with FD correction and the exclusion mask. All maps used thresholds of  $p < 0.001$  (uncorrected for multiple comparisons) at the voxel level and  $p < 0.05$  (FWE-corrected) at the cluster level. FD+, fALFF map with FD correction; FD-, fALFF map without FD correction; mask+, fALFF map with exclusion mask; mask-, fALFF map without exclusion mask

The present study focused only on FC with the thalamus for the purpose of validating the method. However, examination of FC in brain regions other than the thalamus is important to elucidate the effects of anesthetics on brain activity. Although imaging artifacts prevented us from examining frontal activities, changes in FC in whole-brain networks, particularly in the FPN, should be addressed in future studies.

Decreased FC between the thalamus, caudate nucleus and globus pallidus was observed during anesthesia. Previous studies on anesthesia and thalamic-basal ganglia connectivity have reported that sevoflurane anesthesia decreases FC between the thalamus and caudate nucleus [4], that isoflurane decreases glucose metabolism in the thalamus and basal ganglia [22], and that propofol decreases the neural activity of the basal ganglia [23]. However, no previous rs-fMRI studies appear to have mentioned the significance of changes in neural activity in the thalamus and basal ganglia during anesthesia. In contrast, EEG shows that sleep spindles and delta waves predominate under anesthesia. Considering the mechanisms involved in generating those waves, this phenomenon suggests that FC between the thalamus and basal ganglia increases under anesthesia. Meanwhile, periodic suppression of the thalamic circuit is known as the essential element in generating those waves. Thus, we speculate that

such periodic suppression may appear as a decrease in FC between the thalamus and basal ganglia. Alternatively, our results suggest that the cortico-basal ganglia loop through the thalamus may be inhibited under balanced anesthesia with sevoflurane.

Despite the same eye closure condition, decreases in fALFF values were seen in the lingual gyrus, occipital pole, and lateral occipital cortex during anesthesia. Previous studies on anesthesia and activity in visual areas suggest that isoflurane decreases neural activity in the visual cortex [18], that desflurane interferes with visual sensory processing [24], and that volatile anesthetics suppress visual evoked potentials [25–27].

As with findings from previous studies, the present results suggest that anesthesia with sevoflurane results in decreased neural activity in the visual area.

Various limitations to this study need to be kept in mind when interpreting our findings. Variations in anesthesia concentration and image artifacts may have affected the results. We chose transsphenoidal surgery as a relatively less invasive procedure for the brain parenchyma and enrolled 20 patients to this prospective study. However, even in a prospective study, variations due to individual differences are inevitable and will be an issue to be addressed in the future. Although we selected the least invasive surgical

**Table 3** Results of fractional amplitude of low-frequency fluctuations (fALFF) analysis

Comparison	FD	Mask	Clusters (x, y, z)	Size	Peak t value	Brain regions
pre > intra	-	-	+ 12, -56, +30	226	6.91	Precuneus, PC, right cuneus
			+ 58, -20, +28	92	5.25	Right anterior SMG, right postCG
			-46, -26, +30	77	7.14	Left anterior SMG, left postCG, left PO
			-16, -08, +12	76	6.93	Left thalamus, left pallidum, left putamen
			-08, -26, +36	71	7.1	PC
			-20, +14, +52	53	6.53	Left SFG, left midFG
			-40, -12, +30	53	5.51	Left postCG
			+40, -80, +08	47	5.44	Right inferior LOC
			+40, -56, +22	42	5.74	Right AG
			-14, -106, +04	42	5.16	Left OP
			+22, -96, +18	40	5.94	Right OP
			-10, -64, +38	34	5.38	Precuneus
			+18, +14, +50	32	6.68	Right SFG
			+38, -66, +02	30	6.33	Right inferior LOC
			+16, -50, +02	30	4.36	Right LG, right Cereb45
			+40, -82, +06	64	6.66	Right inferior LOC
			+10, -58, +36	60	11.91	Precuneus, PC
			+40, -82, +06	64	6.66	Right inferior LOC
			+10, -58, +36	60	11.91	Precuneus, PC
intra > pre	-	-	+60, +12, -12	251	8.28	Right TP, right anterior MTG, right anterior STG
			+46, -44, -20	251	8.5	Right temporooccipital ITG, right posterior ITG, right Cereb1, right TOFusC, right posterior MTG, right Cereb2
			-46, -68, -22	199	9.99	Left OFusG, left Cereb1, left inferior LOC, left temporooccipital ITG, left TOFusC, left Cereb6
			-08, +22, -24	136	6.24	SubCalC, left FOrb, MedFC
			-64, -08, -22	127	6.53	Left anterior MTG, left posterior MTG, left anterior STG
			-04, +64, -18	97	5.34	left FP, right FP, MedFC
			-48, +08, -32	95	7.69	Left TP
			+54, -22, -38	67	7.18	Right posterior ITG, right posterior TFusC
			-40, -46, -52	61	7.05	left Cereb8
			+48, -42, -14	102	7.16	Right posterior ITG, right temporooccipital ITG, right Cereb1, right TOFusC
			-42, -70, -16	73	6.94	Left inferior LOC, left OFusG, left Cereb1
			+48, -42, -14	102	7.16	Right posterior ITG, right temporooccipital ITG, right Cereb1, right TOFusC
			-42, -70, -16	73	6.94	Left inferior LOC, left OFusG, left Cereb1

\*PC, posterior part of cingulate gyrus; LOC, lateral occipital cortex; SMG, supramarginal gyrus; OP, occipital pole; SFG, superior frontal gyrus; PostCG, postcentral gyrus; LG, lingual gyrus; Cereb, cerebellum; MidFG, middle frontal gyrus; AG, angular gyrus; PO, parietal opercular cortex; TP, temporal pole; ITG, inferior temporal gyrus; SubCalC, subcallosal cortex; OFusG, occipital fusiform gyrus; MTG, middle temporal gyrus; FP, frontal pole; FOrb, frontal orbital cortex; TOFusC, temporal occipital fusiform cortex; MedFC, frontal medial cortex; STG, superior temporal gyrus; TFusC, temporal fusiform cortex; Cereb, cerebellum; pre > intra, brain regions showing significant decrease in fALFF value during anesthesia; intra > pre, brain regions showing significant increase in fALFF value during anesthesia; FD, framewise displacement

cases possible, we could not exclude the effects of surgical invasion. We therefore cannot conclude that the results were exclusive to the effects of anesthesia. In particular, we could not perform network analysis using the whole brain, because we excluded areas in which spatial susceptibility artifacts were observed. In addition, the results may vary depending on the dose of inhaled anesthetics and narcotics used, and the generalizability of results from this study needs to be verified in the future.

In this study, we performed rs-fMRI during neurosurgery and showed results consistent with previous findings indicating the feasibility of intraoperative rs-fMRI during general anesthesia. We were able to evaluate brain function during general anesthesia as close as possible to actual clinical conditions. In addition, we were able to present solutions to the problems of differences in body movements and spatial artifacts compared to awake patients, which are problems when analyzing rs-fMRI during actual neurosurgical procedures.

**Supplementary Information** The online version contains supplementary material available at <https://doi.org/10.1007/s00540-025-03477-y>.

**Acknowledgements** The authors are grateful to Yuichiro Somiya, R.T. (Department of Radiology, Kobe University Hospital, Kobe, Hyogo, Japan) for technical assistance with the MRI experiments, and Moritoki Egi, M.D., Ph.D. (Department of Anesthesia, Kyoto University Hospital, Kyoto, Kyoto, Japan) for useful discussions. We also thank FORTE Science Communications (<https://www.forte-science.co.jp/>) for English language editing. This work is supported by a Grant-in-Aid for Scientific Research from the Japan Society for the Promotion of Science (19K18295).

**Authors' contributions** Research design: Junji Wakabayashi, Yoshitetsu Oshiro, Shigeyuki Kan, Masaaki Kohta, Masaaki Taniguchi, Norihiko Obata, Masako Okada, Eiji Kohmura, Takashi Sasayama, Satoshi Mizobuchi. Conduct of research: Junji Wakabayashi, Yoshitetsu Oshiro, Masaaki Kohta. Patient recruitment: Junji Wakabayashi, Masaaki Kohta, Masaaki Taniguchi. Data collection: Junji Wakabayashi, Masaaki Kohta. Analytical tools: Yoshitetsu Oshiro, Shigeyuki Kan. Data analysis: Junji Wakabayashi, Yoshitetsu Oshiro, Shigeyuki Kan. Writing of paper: Junji Wakabayashi, Yoshitetsu Oshiro, Shigeyuki Kan, Norihiko Obata, Masako Okada, Satoshi Mizobuchi.

**Funding** This study was funded by a Grant-in-Aid for Scientific Research from the Japan Society for the Promotion of Science (19K18295).

**Data availability** The datasets generated during the current study are available from the corresponding author upon reasonable request. A preliminary version of this work was deposited in the Research Square on August 9, 2024 (DOI: <https://doi.org/https://doi.org/10.21203/rs.3.rs-4699067/v1>).

## Declarations

**Competing interests** The all authors declare that they have no conflicts of interest with this work.

## References

- Ramani R, Qiu M, Constable RT. Sevoflurane 0.25 MAC preferentially affects higher order association areas: a functional magnetic resonance imaging study in volunteers. *Anesth Analg*. 2007;105(3):648–55. <https://doi.org/10.1213/01.ane.0000277496.12747.29>.
- Daniel GS, Audrey V, Alain P, Melanie B, Carol DP, Andreas R, Gerhard S, Steven L, Denis J, Vincent B, Rüdiger I. Change in whole brain dynamics and connectivity patterns during sevoflurane- and propofol-induced unconsciousness identified by functional magnetic resonance imaging. *Anesthesiology*. 2019;130:898–911. <https://doi.org/10.1097/ALN.0000000000002704>.
- Palanca BJA, Avidan MS, Mashour GA. Human neural correlates of sevoflurane-induced unconsciousness. *Br J Anaesth*. 2017;119(4):573–82. <https://doi.org/10.1093/bja/aex244>.
- Martuzzi R, Ramani R, Qiu M, Rajeevan N, Constable RT. Functional connectivity and alterations in baseline brain state in humans. *Neuroimage*. 2010;49(1):823–34. <https://doi.org/10.1016/j.neuroimage.2009.07.028>.
- Yashar B, Khaled R, Joy L, Thomas TL. A component based noise correction method (CompCor) for BOLD and perfusion based fMRI. *Neuroimage*. 2007;37(1):90–101. <https://doi.org/10.1016/j.neuroimage.2007.04.042>.
- Ranft A, Golkowski D, Kiel T, Riedel V, Kohl P, Rohrer G, Pientka J, Berger S, Thul A, Maurer M, Preibisch C, Zimmer C, Mashour GA, Kochs EF, Jordan D, Ilg R. Neural correlates of sevoflurane-induced unconsciousness identified by simultaneous functional magnetic resonance imaging and electroencephalography. *Anesthesiology*. 2016;125(5):861–72. <https://doi.org/10.1097/ALN.0000000000001322>.
- Alkire MT, Haier RJ, Fallon JH. Toward a unified theory of narcosis: brain imaging evidence for a thalamocortical switch as the neurophysiologic basis of anesthetic-induced unconsciousness. *Conscious Cogn*. 2000;9(3):370–86. <https://doi.org/10.1006/ccog.1999.0423>.
- Zou QH, Zhu CZ, Yang Y, Zuo XN, Long XY, Cao QJ, Wang YF, Zang YF. An improved approach to detection of amplitude of low-frequency fluctuation (ALFF) for resting-state fMRI: fractional ALFF. *J Neurosci Methods*. 2008;172(1):137–41. <https://doi.org/10.1016/j.jneumeth.2008.04.012>.
- Power JD, Barnes KA, Snyder AZ, Schlaggar BL, Petersen SE. Spurious but systematic correlations in functional connectivity MRI networks arise from subject motion. *Neuroimage*. 2012;59(3):2142–54. <https://doi.org/10.1016/j.neuroimage.2011.10.018>.
- Kim JH, De Asis-Cruz J, Kapse K, Limperopoulos C. Systematic evaluation of head motion on resting-state functional connectivity MRI in the neonate. *Hum Brain Mapp*. 2023;44(5):1934–48. <https://doi.org/10.1002/hbm.26183>.
- Kato S, Bagarinao E, Isoda H, Koyama S, Watanabe H, Maesawa S, Mori D, Hara K, Katsuno M, Hoshiyama M, Naganawa S, Ozaki N, Sobue G. Effects of head motion on the evaluation of age-related brain network changes using resting state functional MRI. *Magn Reson Med Sci*. 2021;20(4):338–46. <https://doi.org/10.2463/mrms.mp.2020-0081>.
- White NS, Alkire MT. Impaired thalamocortical connectivity in humans during general-anesthetic-induced unconsciousness. *Neuroimage*. 2003;19(2 Pt 1):402–11. [https://doi.org/10.1016/S1053-8119\(03\)00103-4](https://doi.org/10.1016/S1053-8119(03)00103-4).
- Palanca BJ, Mitra A, Larson-Prior L, Snyder AZ, Avidan MS, Raichle ME. Resting-state functional magnetic resonance imaging correlates of sevoflurane-induced unconsciousness. *Anesthesiology*. 2015;123(2):346–56. <https://doi.org/10.1097/ALN.0000000000000731>.
- Boveroux P, Vanhauzenhuyse A, Bruno M, Noirhomme Q, Lauwick S, Luxen A, Degueldre C, Plenevaux A, Schnakers C, Phillips C, Brichant J, Bonhomme V, Maquet P, Greicius M, Laureys S, Boly M. Breakdown of within- and between-network resting state functional magnetic resonance imaging connectivity during propofol-induced loss of consciousness. *Anesthesiology*. 2010;113:1038–53. <https://doi.org/10.1097/ALN.0b013e3181f697f5>.
- Schrouff J, Perlberg V, Boly M, Marrelec G, Boveroux P, Vanhauzenhuyse A, Bruno MA, Laureys S, Phillips C, Pelegriani-Issac M, Maquet P, Benali H. Brain functional integration decreases during propofol-induced loss of consciousness. *Neuroimage*. 2011;57(1):198–205. <https://doi.org/10.1016/j.neuroimage.2011.04.020>.
- Greicius MD, Kiviniemi V, Tervonen O, Vainionpaa V, Alahuhta S, Reiss AL, Menon V. Persistent default-mode network connectivity during light sedation. *Hum Brain Mapp*. 2008;29(7):839–47. <https://doi.org/10.1002/hbm.20537>.
- Huang Z, Wang Z, Zhang J, Dai R, Wu J, Li Y, Liang W, Mao Y, Yang Z, Holland G, Zhang J, Northoff G. Altered temporal variance and neural synchronization of spontaneous brain activity in anesthesia. *Hum Brain Mapp*. 2014;35(11):5368–78. <https://doi.org/10.1002/hbm.22556>.

18. Lv P, Xiao Y, Liu B, Wang Y, Zhang X, Sun H, Li F, Yao L, Zhang W, Liu L, Gao X, Wu M, Tang Y, Chen Q, Gong Q, Lui S. Dose-dependent effects of isoflurane on regional activity and neural network function: A resting-state fMRI study of 14 rhesus monkeys: An observational study. *Neurosci Lett*. 2016;611:116–22. <https://doi.org/10.1016/j.neulet.2015.11.037>.
19. Kaike K, Langsjo J, Aalto S, Oikonen V, Sipila H, Teras M, Hinkka S, Metsahon L, Scheinin H. Effect of sevoflurane, propofol, and adjunct nitrous oxide on regional cerebral blood flow, oxygen consumption, and blood volume in humans. *Anesthesiology*. 2003;99:603–13. <https://doi.org/10.1097/0000542-200309000-00015>.
20. Ku SW, Lee U, Noh GJ, Jun IG, Mashour GA. Preferential inhibition of frontal-to-parietal feedback connectivity is a neurophysiologic correlate of general anesthesia in surgical patients. *PLoS ONE*. 2011;6(10): e25155. <https://doi.org/10.1371/journal.pone.0025155>.
21. Lee U, Ku S, Noh G, Baek S, Choi B, Mashour GA. Disruption of frontal-parietal communication by ketamine, propofol, and sevoflurane. *Anesthesiology*. 2013;118(6):1264–75. <https://doi.org/10.1097/ALN.0b013e31829103f5>.
22. Park TY, Nishida KS, Wilson CM, Jaiswal S, Scott J, Hoy AR, Selwyn RG, Dardzinski BJ, Choi KH. Effects of isoflurane anesthesia and intravenous morphine self-administration on regional glucose metabolism ( $[(18)F]FDG$ -PET) of male Sprague-Dawley rats. *Eur J Neurosci*. 2017;45(7):922–31. <https://doi.org/10.1111/ejn.13542>.
23. Martinez-Simon A, Alegre M, Honorato-Cia C, Nunez-Cordoba JM, Cacho-Asenjo E, Troconiz IF, Carmona-Abellan M, Valencia M, Guridi J. Effect of dexmedetomidine and propofol on basal ganglia activity in Parkinson disease: a controlled clinical trial. *Anesthesiology*. 2017;126(6):1033–42. <https://doi.org/10.1097/ALN.0000000000001620>.
24. Lee H, Tanabe S, Wang S, Hudetz AG. Differential effect of anesthesia on visual cortex neurons with diverse population coupling. *Neuroscience*. 2021;458:108–19. <https://doi.org/10.1016/j.neuroscience.2020.11.043>.
25. Hayashi H, Kawaguchi M. Intraoperative monitoring of flash visual evoked potential under general anesthesia. *Korean J Anesthesiol*. 2017;70(2):127–35. <https://doi.org/10.4097/kjae.2017.70.2.127>.
26. Kumar A, Bhattacharya A, Makhija N. Evoked potential monitoring in anaesthesia and analgesia. *Anaesthesia*. 2000;55(3):225–41. <https://doi.org/10.1046/j.1365-2044.2000.01120.x>.
27. Ma J, Xiong W, Guo D, Wang A, Qiao H, Han R. Effects of sevoflurane-propofol-balanced anesthesia on flash visual evoked potential monitoring in spine surgery: a randomized noninferiority trial. *Anesth Analg*. 2022;134(5):1054–61. <https://doi.org/10.1213/ANE.0000000000005742>.

**Publisher's Note** Springer Nature remains neutral with regard to jurisdictional claims in published maps and institutional affiliations.

Springer Nature or its licensor (e.g. a society or other partner) holds exclusive rights to this article under a publishing agreement with the author(s) or other rightsholder(s); author self-archiving of the accepted manuscript version of this article is solely governed by the terms of such publishing agreement and applicable law.